Transcanal Transpromontorial Approach to Lateral Skull Base: Maximal Area of Exposure and Surgical Extensions

Abraam Yacoub[1,2,3], MD; Wilhelm Wimmer[1,2], PhD; Giulia Molinari[1,4], MD, Matteo Alicandri-Ciufelli[4], MD, FEBORL-HNS; Livio Presutti[4], MD; Marco Caversaccio[1,2], MD; Lukas Anschuetz[1,2], MD

[1] Department of Otolaryngology Head and Neck Surgery, Inselspital, University Hospital and University of Bern, Switzerland

[2] Hearing Research Laboratory, ARTORG Center for Biomedical Engineering, University of Bern, Switzerland

[3] Department of Otolaryngology Head and Neck Surgery, Faculty of Medicine, Ain Shams University, Cairo, Egypt

[4] Department of Otolaryngology Head and Neck Surgery, University Hospital of Modena, Italy

Running title

Maximal Exposure in Transpromontorial Approach

Conflict of Interest

The authors declare no conflict of interest

Corresponding Author

Abraam Yacoub

Department of Otolaryngology Head and Neck Surgery, Inselspital, University Hospital and

University of Bern

Freiburgstrasse 15, CH-3010 Bern, Switzerland

Email: abraam.yacoub@gmail.com

Tel: +41316322654

 Fax: +41316324872

Abstract

Objectives/Hypothesis: To determine the possible surgical extensions and maximal area of

exposure (AOE) achievable through the transcanal transpromontorial approach (TTA) to

the internal auditory canal (IAC) and cerebellopontine angle (CPA). We hypothesize a

possible extension of indication for this minimally-invasive approach to the lateral skull

base.

Study design: Experimental anatomical study.

Methods: First, the expanded transcanal transpromontorial approach was carried out in 4

temporal bones to define the anatomical boundaries of the maximal exposure, from two

perspectives, the middle ear and the porus of the IAC. Consecutively, these identified

boundaries were translated on segmented 3D surface models of 32 temporal bone high-

resolution computed tomography scans.

Results: The dissections performed were the basis followed during the determination of the AOE on the segmented 3D surface models. The measurements revealed that the AOE at the middle ear was 152.9 mm^2 +/- 33.6 mm^2, while it was 151.9 mm^2 +/- 24.8 mm^2 at the porus of the IAC. The mean superoinferior and anteroposterior extensions at the middle ear were 14.7 mm +/- 2.5 mm and 16.9 mm +/- 2.5 mm respectively. On the other hand, at the porus of the IAC, the mean superoinferior and anteroposterior extensions were 10.3 mm +/- 1.3mm and 18.5mm +/-1.9mm respectively.

Conclusions: Consistently with the minimally invasive approaches, the AOE is limited; however, if compared to traditional approaches, it appears of considerable size. Our results may assist the surgeon in the selection process of the appropriate candidates to TTA, and to tailor the approach to the disease.

Level of evidence: NA

Introduction

The surgical access to the internal auditory canal (IAC) and the cerebello-pontine angle (CPA) remains under investigation due to its complex anatomy and location at the lateral skull base. The mainly used approaches to treat lesions in these regions are the retrosigmoid, translabyrinthine, and middle cranial fossa. These techniques do not provide direct access to the IAC, as they encroach it from above in the middle cranial fossa approach or from behind in the retrosigmoid and translabyrinthine approaches. Several studies have illustrated the indications, limitations, and possible postoperative complications of these approaches.[1,2]

Recently and after the application of the exclusive endoscopic technique in middle ear surgery, the endoscope was adopted to establish a direct corridor to the IAC and CPA. This technique utilizes the external auditory canal and middle ear landmarks as a direct route to the IAC.[3–5] In 2013, Presutti and his colleagues reported the first clinical case of an intracanalicular cochlear schwannoma excised through an exclusive endoscopic transcanal transpromontorial approach (EndoTTA).[6] After that, Marchioni et al. described the efficacy of the EndoTTA by presenting the first case series of vestibular schwannomas Koos Grade I, II managed with this novel technique.[7]To expand the clinical indications of this approach, the same team introduced the combined endoscopic and microscopic dissection modality in the expanded transcanal transpromontorial approach (ExpTTA) for resection of larger vestibular schwannomas up to Koos grade III.[8,9]

Like the translabyrinthine approach, the transpromontorial surgical technique does not allow hearing preservation, which similarly limits its indication. However, compared to all the traditional approaches, it has several advantages: no or very partial soft tissue dissection, limited drilling of temporal bone, no need for craniotomy, no cerebellar or temporal lobe retraction, a direct and straight view of the surgical target. These features

give the reason to refer to transcanal transpromontorial approaches as minimally invasive. Reports on the rate of post-operative complications and outcomes, such as facial nerve palsy, have confirmed the low morbidity of these approaches.[8,10,11]

However, the indications for a minimal-invasive approach strongly depend on the disease extension, since the management of large lesions inside the CPA are not amendable to this technique. Therefore, it is of utmost importance for the surgeon to be aware of the maximally possible approach extensions in order to appropriately elaborate a case-depending surgical plan. The aim of the present study would be to investigate the maximal surface area exposable using a transcanal transpromontorial approach (TTA) at the level of the middle ear and the porus of the IAC. The provided measurements will refine the determination of the approach indications and limitations and therefore lead to improved preoperative planning and patient counselling.

Materials and Methods

The proposed study was validated by our institutional review board (KEK-BE 2016-00887). To reach our aims, anatomical dissections and measurements on three-dimensional (3D) temporal bone reconstructions were performed.

Anatomical dissections

Four formalin-fixed temporal bones were dissected according to the ExpTTA described by Presutti et al (Figure 1).[4] Zero and 45-degree endoscopes coupled with a high-resolution camera (Karl Storz, Tuttlingen, Germany) and an operating microscope Leica DI C500 (Leica Microsystems IR GmbH) were used to conduct the dissections. The purpose of these dissections was to define and recognize the anatomical boundaries of the maximal area of exposure (AOE) of the surgical approach, from two perspectives: first at the middle

ear referred to as "lateral surgical window", and the second at the porus of the IAC referred to as "medial surgical window". Subsequently, these boundaries were translated on the temporal bone reconstructions.

Three-dimensional temporal bone reconstruction and measurements

High resolution computed tomography scans (HRCTs) of 32 adult temporal bones without pathologies were obtained with a voxel size of 0.156 x 0.156 x 0.2 mm^3 (SOMATOM Definition Edge, Siemens, Erlangen, Germany). The HRCTs data was processed by threshold-based segmentation software (Amira, FEI, France) to create 3D surface models for the temporal bone structures. For each specimen, manual segmentation of the bony labyrinth, facial nerve, internal carotid artery (ICA), jugular bulb (JB), IAC, and cochlear aqueduct (CA) was performed.

To calculate the maximal AOE of the lateral surgical window, six points were determined (Figure 2):

>   1) inferior extent: highest level of the JB
>
>   2) and 3): anterior limit: posterior wall of the ascending petrous ICA at the level of the hypotympanum inferiorly (point 2) and at level of the Eustachian tube orifice superiorly (point 3)
>
>   4) superior extent: geniculate ganglion
>
>   5) and 6) posterior limit: facial nerve at the second genu (point 5), and mastoid segment of the facial nerve, crossing the inferior margin of the tympanic ring (point 6)

The maximal AOE of the approach at the porus of the IAC was determined by the means of another 6 points (Figure 3):

1) superior extent: superior margin of the IAC

2) and 3) posterior extent; posterior margin of the IAC, superiorly at the junction with a perpendicular line along the superior margin of the IAC (point 2), and inferiorly at the junction with a perpendicular line along the medial opening of the CA (point 3)

4) inferior limit: medial opening of the CA.

5) and 6) anterior extent: posterior wall of the ascending petrous ICA. Therefore, a coronal plane demarcating the posterior wall of the ICA was selected (Figure 3C). Point 5 was determined at the junction of that plane with the posterior angle of the petrous bone, while point 6 was determined at the junction of that plane with a perpendicular line along the superior margin of the IAC.

The landmark coordinates were imported into a MATLAB script (The MathWorks Inc., Natick, MA). For each surgical window, a plane was fit to the 6 landmarks using a minimum least squares method. Then, the points were projected orthogonally onto the plane. The projected, coplanar points formed a polygon, which was used to compute the AOE.

Results

The dissections performed on the temporal bones were the basis of the consecutively performed measurements in the segmented 3D-models. The identification of the extreme extensions of the surgical exposure either at the middle ear or towards the CPA allowed the consecutive measurements. From the measurement done on the 32 3D-reconstruced temporal bone reconstructions, the mean area exposed in the middle ear window was 152.9 mm^2 +/- 33.6 mm^2 (range 87.4 – 215.3 mm^2). For the medial window at the IAC porus the mean extension of the surgical window was 151.9 mm^2 +/- 24.8 mm^2 (range 101.3 –201.2 mm^2).

At the level of the middle ear, the mean distance between the geniculate ganglion (point 4) and the JB (point 1) was 14.7 mm +/- 2.5 mm representing the maximal superior-inferior distance of the approach. While the anterior-posterior extension was 16.9 mm +/- 2.5 mm between the posterior wall of the ascending petrous ICA at the orifice of the Eustachian tube (point 3) and the second genu of the facial nerve (point 5). Regarding the superior-inferior extension of the surgical window at the IAC porus, the mean distance between the upper margin of the IAC (point 1) and the medial opening of the CA (point 4) was 10.3 mm +/- 1.3mm. The distance between the posterior limit of the IAC (point 3) and the posterior angle of the petrous bone (point 5) referring as the anterior-posterior extension of the approach was 18.5mm +/-1.9mm.

Discussion

In this study, we describe the maximal area of exposure reachable using the minimal-invasive TTA to the IAC and CPA, based on 3D-reconstructions of healthy temporal bones. A lateral window in the middle ear was defined with a mean extension of 152.9 mm^2 and a medial window at the level of the IAC porus was measured as 151.9 mm^2. These measurements allow an efficient preoperative planning in order to provide a safe procedure tailored to the extent of the disease. Therefore, it is fundamental to define the anatomical limitations of the transpromontorial procedures regarding the maximal exposure achievable with this kind of approach, as provided in this study.

During the last years, the application of the endoscopic technology to the lateral skull base surgery has led to the introduction of the novel TTAs, which can be considered as minimally invasive and direct approaches to the IAC and CPA. Several clinical studies have demonstrated the feasibility and safety of these surgical techniques.[6-11] Since these approaches are still new to the neurotological community, it is important to provide a

quantitative analysis of the maximal AOE. Recently a quantitative study on the AOE and the degree of surgical freedom provided by transcanal approaches to the lateral skull base revealed a mean AOE of 11.1mm^2 for the EndoTTA at the fundus of the IAC, 92.8 mm^2 for the ExpTTA at the fundus and 108.4mm^2 at the porus of the IAC.[12] Compared to the present study, this investigation relied on stereotactic measurements during cadaveric dissection. We observed a considerably larger AOE, both at the middle ear and at the porus of the IAC, indicating the potential for extension when strictly considering the anatomical limits as reported hereby.

In fact, our measurements show a mean lateral window at the middle ear of 152,9 mm^2 and a similar medial window at the IAC porus of 151.9 mm^2. Both windows are of the same size, which implies that the surgical corridor provided by TTA is not cone-shaped, but cylindrical. This moreover signifies, that the landmarks as depicted in the middle ear indicate the limits of the approach at the level of the medial surface of the temporal bone. Therefore, the surgeon can be advised to dissect a similarly sized area from lateral to medial, during the whole course of the surgical corridor. This concept is important during TTA dissection, in order not to progressively restrain the surgical field, oppositely to keep the working area as large as possible, until the porus of the IAC.

Compared to the indirect classical approaches to the IAC and CPA our maximal AOE is certainly smaller but appears of considerable extent (Table 1).[13–17] However, another relevant consideration regards the use of 45-degree lenses during TTA surgery. Despite surgical manipulation is difficult under the angled perspective, especially at the porus of the IAC, the use of angled endoscopes could enlarge the actual visible area and thus provide the surgeon additional information from otherwise hidden zones. This could be helpful both during the access to the IAC for the identification of anatomical landmarks to further guide the surgical steps, and after exposure of the IAC and tumor removal, to

check the CPA area. Hitherto, appropriate longed and curved instruments to operate in depth and "around the corner" in the CPA are lacking; further technical development may meet such needs and thus increase the surgical possibilities of transcanal approaches.

In order to correctly interpret our results, it should be underlined that the selected landmarks for measurements are those theoretically reachable during the most extended surgical access possible. The lateral and medial windows have been set up as a simulation of the surgical field where the anatomical boundaries are skeletonized and exposed at their maximum. The additional measurements at the middle ear showed that the supero-inferior and the antero-posterior extensions were 14.7 mm and 16.9 mm, respectively. This further clarifies the effect of inclination of the JB and ICA at the middle ear on the surgical extension of the approach. Master and colleagues have recently investigated this topic in exclusive endoscopic TTA, suggesting that the anatomic variability in the position of ICA and JB especially, can affect the surgical access and should be preoperatively assessed to predict the feasibility of the approach and the fundostomy size.[18]The jugular bulb position in the tympanic cavity and its possible dehiscence may influence its management during TTA, as in open approaches,[19] and a highly riding jugular bulb has been reported as a relative contraindication to TTA surgery.[20] Anatomical variants of the ICA have also been described, advocating for routine preoperative evaluation of this arterial segment in relation to the middle ear and the Eustachian tube before a number of surgical procedures.[21,22]

On the other hand at the porus of the IAC, the supero-inferior extension or the mean distance between the upper margin of the IAC to the medial opening of the CA was 10.3 mm. All this anatomical variability influences the approach extensions and sometimes adds furthermore to the approach limitations. A possible strategy to enhance the surgical planning would be the generation of semi-automatic 3D models of the patient's data in

order to visualize and measure the available AOE from case to case. These models would make possible to define the relationship of the anatomical landmarks with the target lesion, allowing for a better preoperative awareness of the working area. The application of image-guided navigation technology in lateral skull base is relatively new, mainly because the higher accuracy requirements of this region have limited its development.[23,24] Recently a navigation solution with submillimeter accuracy was successfully applied to middle ear and lateral skull base, using different registration strategies.[25] The intraoperative use of such navigation system during TTA surgery would offer a superior spatial orientation, facilitating the dissection of the trajectory to the IAC and CPA. It is likely that this tool may increase the safety and efficacy of transcanalar approaches, which allow a limited AOE, as highlighted by our results. However, the role of image-guided navigation with submillimeter-scale accuracy in TTA has yet to be investigated by further clinical studies.

Conclusion

A quantitative evaluation of the mean AOE of the surgical field obtained through TTA to the IAC and CPA is provided by this study, according to the measurements on 3D temporal bone reconstruction models. Consistently with the minimally-invasiveness of transcanal approaches, the AOE is limited; however, if compared to traditional approaches, it appears of considerable size. Our results may assist the surgeon in the selection process of the appropriate candidates to TTA, and to tailor the approach to the disease.

References

1. Ansari SF, Terry C, Cohen-Gadol AA. Surgery for vestibular schwannomas: a systematic review of complications by approach. *Neurosurg Focus.* 2012;33(3): E14.

2. Bennett M, Haynes DS. Surgical approaches and complications in the removal of vestibular schwannomas. *Neurosurg Clin N Am.* 2008;19(2):331-343.

3. Komune N, Matsuo S, Miki K, Rhoton AL. The endoscopic anatomy of the middle ear approach to the fundus of the internal acoustic canal. *J Neurosurg.* 2016;126(6):1974-1983.

4. Presutti L, Bonali M, Marchioni D, et al. Expanded transcanal transpromontorial approach to the internal auditory canal and cerebellopontine angle: a cadaveric study. *Acta Otorhinolaryngol Ital.* 2017;37(3):224-230.

5. Marchioni D, Alicandri-Ciufelli M, Mattioli F, et al. From external to internal auditory canal: surgical anatomy by an exclusive endoscopic approach. *Eur Arch Oto-Rhino-Laryngology.* 2013;270(4):1267-1275.

6. Presutti L, Alicandri-Ciufelli M, Cigarini E, Marchioni D. Cochlear schwannoma removed through the external auditory canal by a transcanal exclusive endoscopic technique. *Laryngoscope.* 2013;123(11):2862-2867.

7. Marchioni D, Alicandri-Ciufelli M, Rubini A, Masotto B, Pavesi G, Presutti L. Exclusive endoscopic transcanal transpromontorial approach: a new perspective for internal auditory canal vestibular schwannoma treatment. *J Neurosurg.* 2016;126(1):98-105.

8. Presutti L, Alicandri-Ciufelli M, Bonali M, et al. Expanded transcanal transpromontorial approach to the internal auditory canal: Pilot clinical experience. *Laryngoscope*. 2017;127(11):2608-2614.

9. Marchioni D, Carner M, Soloperto D, et al. Expanded Transcanal Transpromontorial Approach: A Novel Surgical Technique for Cerebellopontine Angle Vestibular Schwannoma Removal. *Otolaryngol Head Neck Surg*. 2018;158(4):710-715.

10. Marchioni D, De Rossi S, Soloperto D, Presutti L, Sacchetto L, Rubini A. Intralabyrinthine schwannomas: a new surgical treatment. *Eur Arch Otorhinolaryngol*. 2018;275(5):1095-1102.

11. Marchioni D, Soloperto D, Masotto B, et al. Transcanal Transpromontorial Acoustic Neuroma Surgery: Results and Facial Nerve Outcomes. *Otol Neurotol*. 2018;39(2):242-249.

12. Anschuetz L, Presutti L, Schneider D, et al. Quantitative Analysis of Surgical Freedom and Area of Exposure in Minimal-Invasive Transcanal Approaches to the Lateral Skull Base. *Otol Neurotol*. 2018;39(6):785-790.

13. Hsu FPK, Anderson GJ, Dogan A, et al. Extended middle fossa approach: quantitative analysis of petroclival exposure and surgical freedom as a function of successive temporal bone removal by using frameless stereotaxy. *J Neurosurg*. 2009;100(4):695-699.

14. Siwanuwatn R, Deshmukh P, Figueiredo E, Crawford N, Spetzler R, Preul M. Quantitative analysis of the working area and angle of attack for the retrosigmoid, combined petrosal, and transcochlear approaches to the petroclival region. *J Neurosurg*. 2006;104(1):137-142.

15. Zador Z, De Carpentier J. Comparative Analysis of Transpetrosal Approaches to the Internal Acoustic Meatus Using Three-Dimensional Radio-Anatomical Models. *J Neurol Surgery, B Skull Base*. 2015;76(4):310-315.

16. Tang CT, Kurozumi K, Pillai P, Filipce V, Chiocca EA, Ammirati M. Quantitative analysis of surgical exposure and maneuverability associated with the endoscope and the microscope in the retrosigmoid and various posterior petrosectomy approaches to the petroclival region using computer tomograpy-based frameless stereotaxy. *Clin Neurol Neurosurg*. 2013;115(7):1058-1062.

17. Horgan MA, Anderson GJ, Kellogg JX, et al. Classification and quantification of the petrosal approach to the petroclival region. *J Neurosurg*. 2009;93(1):108-112.

18. Master A, Hamiter M, Cosetti M. Defining the Limits of Endoscopic Access to Internal Auditory Canal. *J Int Adv Otol*. 2016;12(3):298-302.

19. Sennaroglu L, Slattery WH. Petrous anatomy for middle fossa approach. *Laryngoscope*. 2003;113(2):332-342.

20. Kempfle J, Kozin ED, Remenschneider AK, Eckhard A, Edge A, Lee DJ. Endoscopic Transcanal Retrocochlear Approach to the Internal Auditory Canal with Cochlear Preservation: Pilot Cadaveric Study. *Otolaryngol Head Neck Surg*. 2016;154(5):920-923.

21. Hasebe S, Sando I, Orita Y. Proximity of carotid canal wall to tympanic membrane: A human temporal bone study. *Laryngoscope*. 2003;113(5):802-807.

22. Bergin M, Bird P, Cowan I, Pearson JF. Exploring the critical distance and position relationships between the Eustachian tube and the internal carotid artery. *Otol Neurotol*. 2010;31(9):1511-1515.

23. Rathgeb C, Anschuetz L, Schneider D, et al. Accuracy and feasibility of a dedicated image guidance solution for endoscopic lateral skull base surgery. *Eur Arch Otorhinolaryngol*. 2018;275(4):905-911. doi:10.1007/s00405-018-4906-7

24. Zhou C, Anschuetz L, Weder S, et al. Surface matching for high-accuracy registration of the lateral skull base. *Int J Comput Assist Radiol Surg*. 2016;11(11):2097-2103.

25. Schneider D, Hermann J, Gerber KA, et al. Noninvasive Registration Strategies and Advanced Image Guidance Technology for Submillimeter Surgical Navigation Accuracy in the Lateral Skull Base. *Otol Neurotol*. 2018;39(10):1326-1335.

Table 1. Comparison of area of exposure provided by the approaches to the internal audioty canal/cerebello-pontine angle and petro-clival region.

*Maximal exposure at the petro-clival /brainstem region, according to microscopic view.

Approach	Exposed area (mm^2)	SD ($\pm$ mm^2)
Middle fossa		
Hsu (2004)[13]	128	47
Retrosigmoid		
Siwanuwatn (2006)[14]		
Petroclival window	292.4	59.9
Brainstem window	177.2	54.2
Tang (2006)[16]*	235	25
Retrolabyrinthine		
Zador (2015)[15]	140.30	30.92
Tang (2013)[16]*	99	112
Horgan (2000)[17]	108	51
Translabyrinthine		
Zador (2015)[15]	245.3	44.27
Transcochlear		
Tang (2013)[16]*	502	190
Horgan(2000)[17]	514	78
Siwanuwatn(2006)[14]		
Petroclival window	755.6	130.1
Brainstem window	399.3	68.2
Transcrusal		
Zador (2015)1[15]	181.63	38.55
Horgan(2000)[17]	449	71
Transotic		
Horgan(2000)[17]	476	62
Combined petrosal		
Siwanuwatn (2006)[14]		
Petroclival window	354.1	60.3
Brainstem window	289.7	69.9
Transcanal transpromontorial		

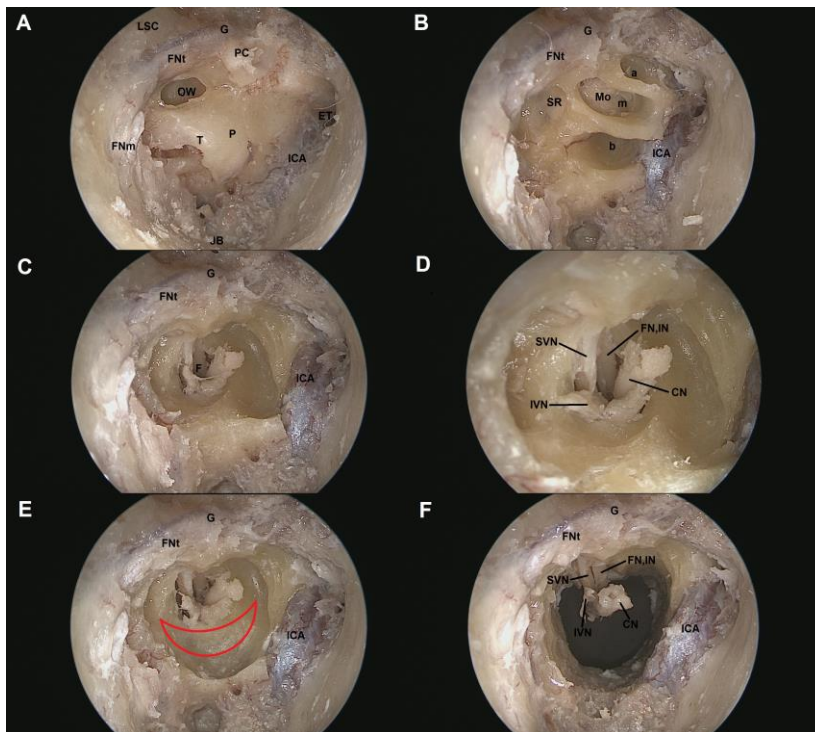|		
Lateral window	152.9	33.6
Medial window	151.9	24.8

Figure Legends

Figure 1: Dissection steps of the expanded transcanal transpromontorial approach to the internal auditory canal and the cerebello-pontine angle (CPA). Photographs were taken by 0° angle endoscope during dissection of a right-sided temporal bone.

Panel A: View after the maximal exposure at the middle ear. B: Opening of the cochlear turns. C, D: Fundus of the internal auditory canal and distribution of the facial and vestibulocochlear nerves. E: Photograph illustrating the technique of the widening of the transcanal corridor to the CPA. The red crescent indicates the bony area followed during the expansion. F: After the approach expansion to the CPA.

a, apical turn of the cochlea; b, basal turn of the cochlea; CN, cochlear nerve; F, fundus of the internal auditory canal; FNm, mastoid segment of the facial nerve; FNt, tympanic segment of the facial nerve; FN+IN, facial nerve and intermediate nerve; G, geniculate

ganglion; ICA, internal carotid artery; IVN, inferior vestibular nerve; JB, jugular bulb; LSC, lateral semicircular canal; m, middle turn of the cochlea; Mo, modiolus; P, promontory; PC, processus cochleariformis; SR, spherical recess; SVN, superior vestibular nerve.
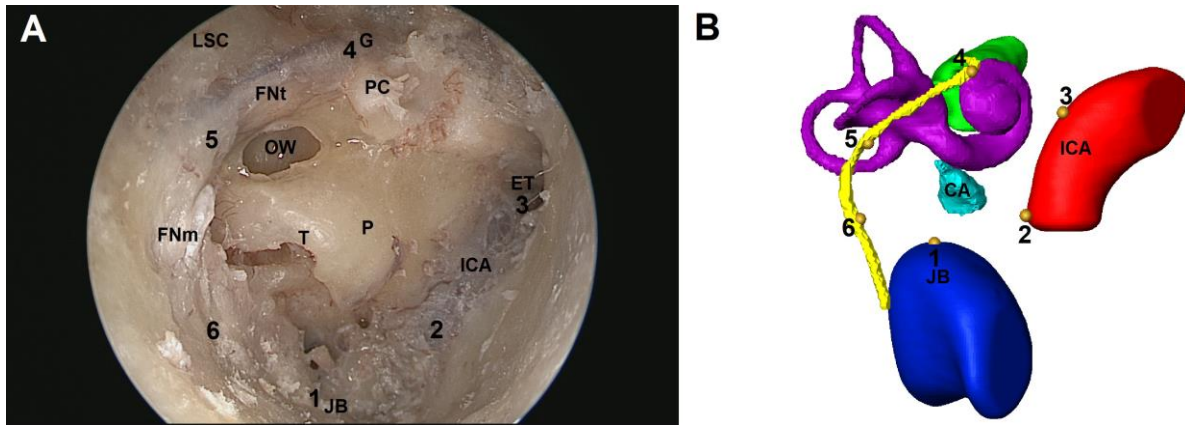

Figure 2: Area of exposure at the middle ear (Lateral surgical window)

Panel A: Endoscopic photograph demonstrating the boundaries of the maximal exposure at the middle ear. B: 3-dimensional reconstructed surface model of a right temporal bone showing the method of calculation of the area of exposure at the lateral window. Boundaries of the surgical exposure that could be obtained from the temporal bone dissections were translated on the obtained reconstructions.

CA, cochlear aqueduct; ET, eustachian tube; FNm, mastoid segment of the facial nerve; FNt, tympanic segment of the facial nerve; G, geniculate ganglion; ICA, internal carotid artery; JB, jugular bulb; LSC, lateral semicircular canal; OW, oval window; P, promontory; PC, processus cochleariformis; T, tegmen of the round window.
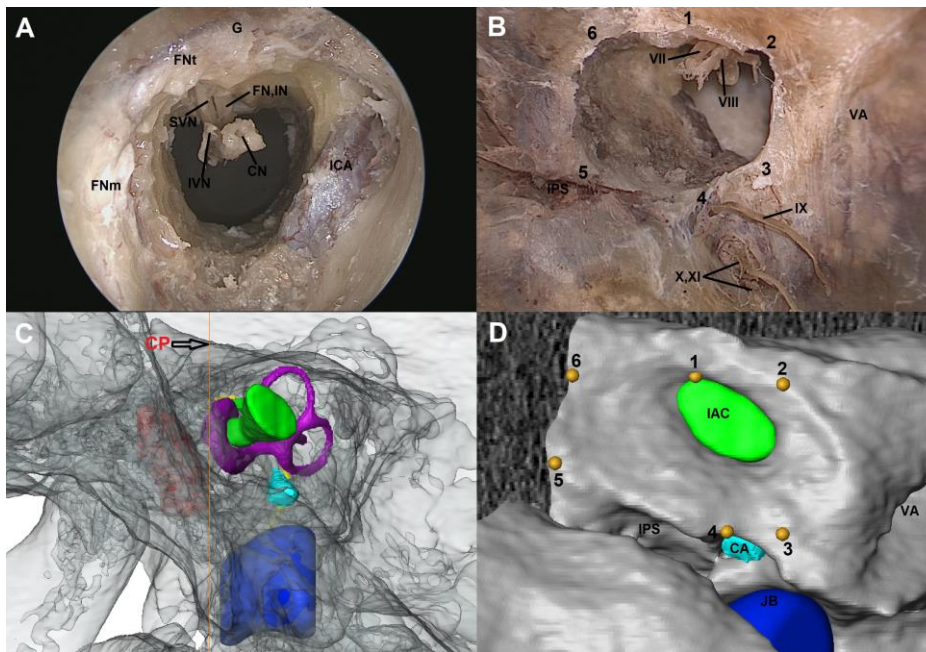
Figure 3: Area of exposure at the porus of the internal auditory canal (Medial surgical window)

Panel A, B: Dissection photographs showing the boundaries of the maximal exposure at the medial surgical window. A: Endoscopic photograph taken by 0° angle endoscope through the external auditory canal. B: Photograph for the posterior surface of the petrous bone demonstrating the relationship between the obtained window with the surrounding anatomical structures.

C, D: 3-dimensional reconstructed surface model of a right temporal bone structures clarifying the method of calculation of the area of exposure. C: Determination of the coronal plane, which demarcates the posterior wall of the ascending petrous ICA. This plane was used as an anterior limit for the exposure. D: Translation of the boundaries of the surgical exposure that could be obtained from the temporal bone dissections on the temporal bone reconstructions.

CA, cochlear aqueduct; CP, coronal plane demarcating the posterior wall of the ascending petrous ICA; FNt, tympanic segment of the facial nerve; G, geniculate ganglion; IAC, internal auditory canal; ICA, internal carotid artery; JB, jugular bulb; IPS, inferior petrosal

sulcus; VA, vestibular aqueduct; VII, facial nerve; VIII, vestibulocochlear nerve; IX,

glossopharyngeal nerve; X, vagus nerve; XI, accessory nerve.